


# An expanded impedance control scheme for slosh-free liquid transfer by a dual-arm cooperative robot

Journal of Vibration and Control  
2020, Vol. 0(0) 1–14  
© The Author(s) 2020  
Article reuse guidelines:  
[sagepub.com/journals-permissions](https://sagepub.com/journals-permissions)  
DOI: 10.1177/1077546320966208  
[journals.sagepub.com/home/jvc](https://journals.sagepub.com/home/jvc)  


Babak Naseri Soufiani<sup>1</sup> and Mehmet Arif Adli<sup>1</sup>

## Abstract

The use of robots has been rapidly spreading in different daily applications. The transport of liquids by robot arms without causing any slosh is one of such applications which has recently taken the attention of researchers. Liquid transfer by dual-arm robots causes challenging problems because, in the process of dual-arm cooperation, a closed kinematic chain is formed and a set of constraints appears in motion, which increases the complexity of the process. In this study, an expanded impedance control was proposed for a dual-arm cooperative robot to achieve high speed for the transfer of a liquid-filled cylindrical container without sloshing. The impedance control method provides efficient results in controlling multi-robot interactions. However, a conventional impedance control is incapable of suppressing the slosh during liquid transfer. Therefore, in this study, we expand the impedance control by introducing a slosh suppression term, which leads to suppressing the slosh successfully during the transport of a liquid container. The effectiveness of the proposed controller was demonstrated for liquid transfer in a 2-D plane.

## Keywords

Liquid slosh, slosh suppression, dual-arm cooperative robot, closed kinematic chain, impedance control

## 1. Introduction

The roles and functions of robots are rapidly increasing. In the near future, in addition to the current functions they perform, robots will be used for many other human tasks that require dexterity. Therefore, various studies which imitate skillful functions of human beings are being carried out. In this context, the studies on liquid handling robots have begun to attract the attention of researchers (Aribowo et al., 2010; Reyhanoglu and Hervas, 2013; Tzamtzi et al., 2007).

Dual-arm cooperative robots are mostly used for tasks that cannot be easily executed by a single robot arm. Compared with single-arm robots, dual-arm cooperative robots have significant advantages such as manipulating/transporting large or heavy loads, dexterity, agility, and human-like control over their environment. However, in the process of dual-arm cooperation, the closed kinematic chain is formed, and a set of constraints appears in motion, which increases the complexity of the process. Therefore, in comparison with single-arm manipulation, dual-arm manipulation needs more advanced, elaborate, and viable control approaches. A considerable amount of literature has been published on dual-arm robots in connection with their applications, modeling, and control (Caccavale et al., 2008; Ren et al., 2016; Smith et al., 2012; Wang et al., 2015).

During the transfer of a liquid-filled container, as a result of acceleration and deceleration, oscillation of the free surface of the liquid or sloshing occurs. Sloshing liquid creates undesirable forces and moments that affect the performance of the fast liquid transfer system. Thus, it can be dangerous during the transportation of especially hazardous liquids such as acid, molten metal, fuel, and other explosive fluids. Hence, the sloshing needs to be suppressed while maintaining a high-speed transfer.

In the literature, there are various studies on active and passive methods to prevent sloshing. The passive methods, such as baffles, bladders, and partitions inside the container, reduce the adverse effects of sloshing by damping kinetic energy, which is generated by the movement of the fluid in the container (Hasheminejad et al., 2014; Jung et al., 2012; Panigrahy et al., 2009; Xue et al., 2012). However, in

---

Mechanical Engineering Department, Gazi University, Turkey

Received: 23 April 2020; accepted: 20 September 2020

### Corresponding author:

Mehmet Arif Adli, Mechanical Engineering Department, Gazi University, Eti Mah. Yükseliş Sok., Maltepe, Ankara 06500, Turkey.  
Email: [arif.adli@gazi.edu.tr](mailto:arif.adli@gazi.edu.tr)

experimental studies, it was observed that passive methods could not completely suppress sloshing. This is mainly because the kinetic energy of the liquid is reduced, but the energy cannot be completely suppressed. Therefore, researchers have focused on active methods. Active slosh control approaches to move liquid-filled containers have been proposed for robotic systems and space vehicles. To prevent liquid sloshing, various models have been developed, and the most commonly used equivalent models in the literature are “pendulum” (Aribowo et al., 2010; Kurode et al., 2013; Tzamtzi et al., 2007; Yano and Terashima, 2001) and “multiple mass-spring” models (Pridgen et al., 2010; Reyhanoglu and Hervas, 2012, 2013).

There are various control algorithms which have been used by researchers to handle the slosh suppression problem during liquid transfer. Commonly used control algorithms are Proportional–Integral–Derivative control (Tzamtzi et al., 2007), Proportional–Derivative control (Kim and Choi, 2000), Linear–Quadratic–Integral optimal control (Hamaguchi et al., 1994),  $H_\infty$  feedback control (Yano and Terashima, 2001), Lyapunov-based feedback control (Reyhanoglu and Hervas, 2013), integral sliding mode control (Thakar et al., 2012), sliding mode control (Bandyopadhyay et al., 2009; Kurode et al., 2013), and input shaping control (Aribowo et al., 2010). These controllers aim to keep the liquid level or angle of the container at a certain level to suppress sloshing. In all these studies in which the liquid transfer is carried out by a single robot or done as a one-dimensional movement, the developed controllers are based on position control and do not require to use any force feedback. However, carrying liquid objects by a cooperative dual-arm robot needs to control both position and interaction forces between the two arms.

In our previous study, LQR and pole placement control techniques were applied to eliminate the slosh during liquid transport by obtaining the nonlinear dynamics of dual-arm cooperative robots and liquid slosh (Naseri Soufiani and Adli, 2020). In this study, an appropriate controller for two cooperative robot arms that can perform a slosh-free transfer of liquids was developed. Contrary to the tasks done by a single robot arm, the controller design is quite complicated in general for the tasks done by two robot arms cooperatively. This is mainly because of the interaction of both the position and the force between two coordinating arms. There are various studies concerning cooperative transport or manipulation of rigid or flexible objects by two robot arms (Adli and Hanafusa, 1993; Adli et al., 1991; Al-Yahmadi et al., 2007; Caccavale et al., 2008; Moosavian and Papadopoulos, 2010). However, to the best of our knowledge, there are no studies in the literature that deal with the control of dual-arm cooperative transfer of liquids, which requires a much more complicated control algorithm.

The impedance control is one of the methods used for force and position control by adjusting the mechanical impedance of the end-effector to external forces (Yoshikawa, 1990). This method has been utilized in many robotic applications, especially when there is a robot–robot or human–robot interaction. For instance, it is quite widely used in rehabilitation robots where human–robot interaction is inevitable (Akdoğan and Adli, 2011; Hu et al., 2012; Tsoi and Xie, 2009).

Impedance control, instead of just regulating the force and position directly, regulates the relationship between the force and “position–velocity–acceleration” of a robot arm which is in contact with objects or environment while taking the nonlinear dynamics of the systems involved into account. With the impedance control, the robot arms display a quite similar behavior with the living beings while interacting with a dynamic environment.

## 2. System modeling

Consider the dual-arm cooperative system handling a liquid-filled cylindrical container. The schematic diagram of cooperative robots (each robot has six degrees of freedom) and the liquid container is illustrated in Figure 1. The grasp between the end-effectors of the robot and container handles was modeled as a passive revolute joint. The arms are driven by actuators, which are placed at the joints that were shown by the filled circles (active joints) in the figure. For the ease of the analysis, four kinds of coordinate frames were utilized, where  $\sum B$  denotes the base coordinate frame (reference frame),  $\sum R1$  and  $\sum R2$  are the coordinate frames attached to the end-effectors of Robot 1 and Robot 2, respectively.  $\sum G$  is the object frame which was attached to the “mass center” of the container and rigid portion of the liquid (i.e., nonsloshing part of the liquid), which is assumed to move together with the container as a single rigid mass. The details are explained in Section 2.2.

### 2.1. Kinematics of the system

During dual-arm cooperation, a closed kinematic chain is formed by grasping the container with two robots. The positions and orientations of the two robots must satisfy a set of constraints during the motion. Referring to Figure 1, the position constraints can be expressed as follows (Adli et al., 1995)

$$\phi_i(\mathbf{r}, \mathbf{q}_i) = \mathbf{r}_G + {}^B_G\mathbf{R}\mathbf{p}_i - \mathbf{r}_i = \mathbf{0} \quad (1)$$

where  $\mathbf{r} = [\mathbf{r}_G^T \ \Theta^T]^T$  denotes the position and orientation vector of the container,  $\mathbf{r}_G = [x \ y \ z]^T$  is the center of the mass of the rigid part,  $\mathbf{q}_i$  is robots' joint angles,  ${}^B_G\mathbf{R}$  is the rotation matrix relating the base coordinate frame  $\sum B$  to the

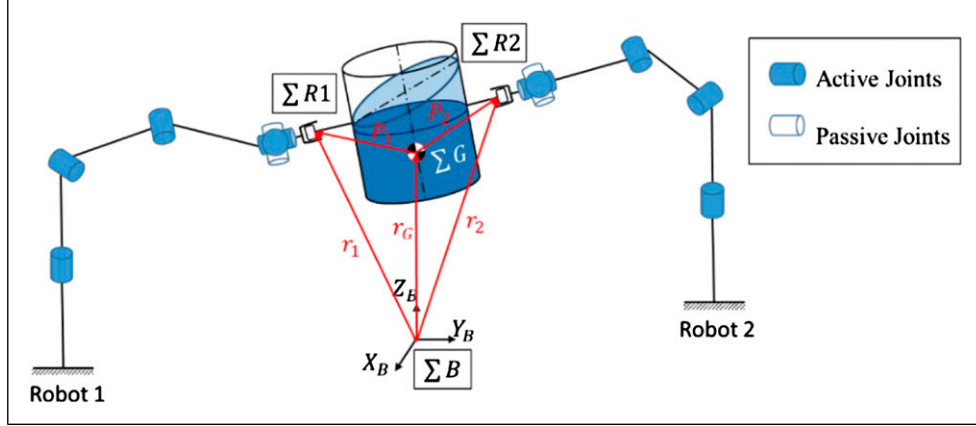


**Figure 1.** Dual-arm cooperative robot carrying liquid-filled container.

object coordinate frame  $\Sigma G$ , and  $\mathbf{P}_i$  is the position vector from the center of the mass of the object to  $i$ th robot end-effector. Taking the derivative of equation (1) with respect to time yields

$$\dot{\Phi}_i = \frac{\partial \Phi_i}{\partial \mathbf{r}} \dot{\mathbf{r}} + \frac{\partial \Phi_i}{\partial \mathbf{q}_i} \dot{\mathbf{q}}_i = \mathbf{0} \quad (2)$$

$$\dot{\mathbf{q}}_i = -\left(\frac{\partial \Phi_i}{\partial \mathbf{q}_i}\right)^{-1} \left(\frac{\partial \Phi_i}{\partial \mathbf{r}}\right) \dot{\mathbf{r}} \quad (3)$$

$$\mathbf{J}_i = \mathbf{J}_{ai}^{-1} \mathbf{J}_{oi} \quad (4)$$

where  $\mathbf{J}_{ai} = -(\partial \Phi_i / \partial \mathbf{q}_i)$  and  $\mathbf{J}_{oi} = (\partial \Phi_i / \partial \mathbf{r})$ . As it is assumed that Jacobian matrix of each robot is invertible, the vector of joint velocities can be expressed as the function of the object velocity.

$$\dot{\mathbf{q}}_i = \mathbf{J}_i \dot{\mathbf{r}} \quad (5)$$

By differentiating equation (5), acceleration relation can be obtained as follows

$$\ddot{\mathbf{q}}_i = \mathbf{J}_i \ddot{\mathbf{r}} + \dot{\mathbf{J}}_i \dot{\mathbf{r}} \quad (6)$$

## 2.2. Dynamics of the system

The liquid slosh dynamic is modeled as an equivalent mechanical model in the form of a simple pendulum. This equivalent mechanical model consists of a rigid mass and a set of pendulum masses, where each pendulum mass represents an individual sloshing mode (Ibrahim, 2005). The viscosity of the liquid is considered as a damper.

While constructing the equivalent mechanical model of the slosh, the following assumptions listed in Ibrahim, 2005 were adopted:

1. Not only the equivalent masses but also the moments of the inertia need to be preserved.
2. For tiny oscillations, the center of the gravity has to remain the same.
3. The system must both have the same modes of oscillations and generate the same damping forces.
4. The force and moment components have to be equivalent to the ones produced by the actual system under certain excitation.

Using Lagrange's formulation, the equations of the motion of the system shown in Figure 2 can be defined in the following matrix form in task space

$$\mathbf{M}_o(\mathbf{X}_o) \ddot{\mathbf{X}}_o + \mathbf{C}_o(\dot{\mathbf{X}}_o, \mathbf{X}_o) \dot{\mathbf{X}}_o + \mathbf{G}_o(\mathbf{X}_o) = \sum_{i=1}^2 \mathbf{J}_{oi}^T \mathbf{F}_i \quad (7)$$

where  $\mathbf{M}_o(\mathbf{X}_o) \in \mathcal{R}^{(6+2n) \times (6+2n)}$  denotes the inertia matrix; the vector  $\mathbf{C}_o(\dot{\mathbf{X}}_o, \mathbf{X}_o) \in \mathcal{R}^{(6+2n)}$  includes the damping force due to viscosity of the liquid, Coriolis effect, and others nonlinear terms;  $\mathbf{G}_o(\mathbf{X}_o) \in \mathcal{R}^{(6+2n)}$  is the gravitational force;  $\mathbf{J}_{oi}^T \in \mathcal{R}^{(6+2n) \times 6}$  represents Jacobian matrix; and  $\mathbf{F}_i \in \mathcal{R}^6$  are the force and moment vectors applied to the object by the robot end-effectors.  $\mathbf{X}_o = [\mathbf{x}_o^T \ \Psi^T]^T \in \mathcal{R}^{(6+2n)}$  denotes the vector of position and orientation of the liquid-filled container. Here,  $\mathbf{x}_o = [x \ y \ z \ \theta_x \ \theta_y \ \theta_z]^T \in \mathcal{R}^6$  is the vector of position and orientation of the rigid portion and  $\Psi = [\psi_1 \ \phi_1 \ \psi_2 \ \phi_2 \dots \ \psi_n \ \phi_n]^T \in \mathcal{R}^{2n}$ , and  $n$  is the number of spherical pendulums corresponding to slosh modes.

The dynamic model of two robot arms in joint space can be written in the following form

$$\mathbf{M}_{Ri}(\mathbf{q}_{Ri})\ddot{\mathbf{q}}_{Ri} + \mathbf{C}_{Ri}(\mathbf{q}_{Ri}, \dot{\mathbf{q}}_{Ri}) + \mathbf{G}_{Ri}(\mathbf{q}_{Ri}) = \boldsymbol{\tau}_{Ri} + \mathbf{J}_{Ri}^T \mathbf{F}_i, \quad (i=1, 2) \quad (8)$$

where  $\mathbf{M}_{Ri}(\mathbf{q}_{Ri}) \in \mathcal{R}^{6 \times 6}$  is the symmetric positive definite inertial matrix of the  $i$ th robot,  $\mathbf{C}_{Ri}(\mathbf{q}_{Ri}, \dot{\mathbf{q}}_{Ri}) \in \mathcal{R}^6$  represents the vector of Coriolis and centrifugal forces and nonlinear terms,  $\mathbf{G}_{Ri}(\mathbf{q}_{Ri}) \in \mathcal{R}^6$  is the vector of gravitational forces,  $\boldsymbol{\tau}_{Ri} \in \mathcal{R}^6$  is the vector of applied joint torques,  $\mathbf{F}_i \in \mathcal{R}^6$  is the vector of forces and moments exerted by the robot end-effectors,  $\mathbf{J}_{Ri}^T \in \mathcal{R}^{6 \times 6}$  is a matrix expressing the Jacobian matrix of the robots, and  $\mathbf{q}_{Ri} \in \mathcal{R}^6$  denotes the vector of joint angle of each manipulator. The subscript  $i$  is used to represent the left and right robot arms.

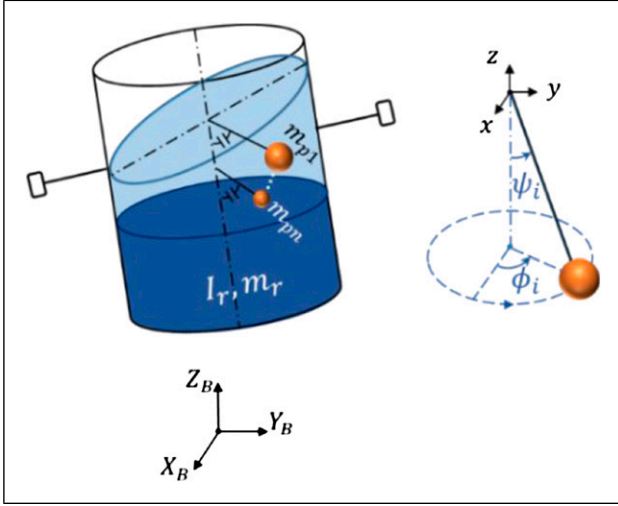


**Figure 2.** Equivalent mechanical model of liquid slosh.

Deriving  $\mathbf{F}_i$  from equation (7) and substituting into (8), the dynamics of the two robot arms can be rewritten as

$$\begin{aligned} \boldsymbol{\tau}_{R1} = & \mathbf{M}_{R1}(\mathbf{q}_{R1})\ddot{\mathbf{q}}_{R1} + \mathbf{C}_{R1}(\mathbf{q}_{R1}, \dot{\mathbf{q}}_{R1}) + \mathbf{G}_{R1}(\mathbf{q}_{R1}) \\ & + \mathbf{J}_{R1}^T (\mathbf{J}_{o1}^T)^{-1} [\mathbf{M}_o \ddot{\mathbf{X}}_o + \mathbf{C}_o(\mathbf{X}_o, \dot{\mathbf{X}}_o) + \mathbf{G}_o(\mathbf{X}_o) + \mathbf{J}_{o2}^T \mathbf{F}_2] \end{aligned} \quad (9)$$

$$\begin{aligned} \boldsymbol{\tau}_{R2} = & \mathbf{M}_{R2}(\mathbf{q}_{R2})\ddot{\mathbf{q}}_{R2} + \mathbf{C}_{R2}(\mathbf{q}_{R2}, \dot{\mathbf{q}}_{R2}) + \mathbf{G}_{R2}(\mathbf{q}_{R2}) \\ & + \mathbf{J}_{R2}^T (\mathbf{J}_{o2}^T)^{-1} [\mathbf{M}_o \ddot{\mathbf{X}}_o + \mathbf{C}_o(\mathbf{X}_o, \dot{\mathbf{X}}_o) + \mathbf{G}_o(\mathbf{X}_o) + \mathbf{J}_{o1}^T \mathbf{F}_1] \end{aligned} \quad (10)$$

### 3. Expanded impedance control

Conventional impedance control is an approach to the control of the dynamic interaction between a manipulator and its environment. This control has been designed for rigid or flexible objects, whereas in this study, the object (a liquid carrying container) cannot be assumed as rigid or flexible. Therefore, the effect of forces due to sloshing liquid is not taken into consideration in the conventional impedance control, and the effect of these forces cannot be successfully suppressed.

During the transport, the motion of the container causes the liquid inside the container to slosh. This, in turn, leads to the formation of undesirable forces. Thus, the effect of these undesirable forces which behave as a disturbance should be eliminated.

In this study, we proposed an expanded impedance control that includes a slosh suppression term  $\mathbf{K}_{d\psi}(\boldsymbol{\Psi} - \boldsymbol{\Psi}_d)$ , which assumes the slosh as an external force that is applied to the container. Using this in the impedance control scheme leads to the elimination of the effects of the slosh rapidly, by forcing the container and liquid together to behave as a rigid

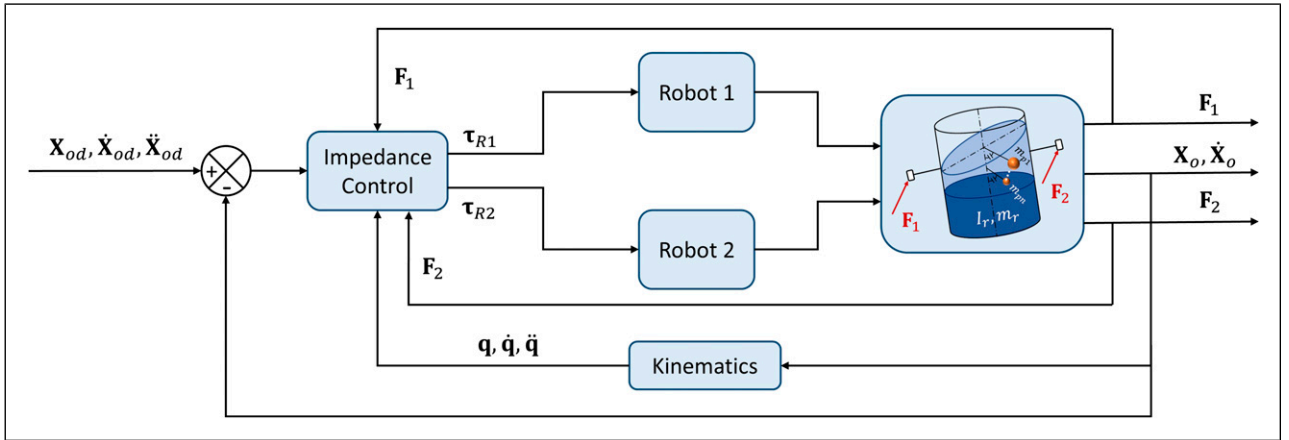


**Figure 3.** Expanded impedance control block diagram.

**Figure 4.** (a) Dual-arm cooperative robot carrying liquid-filled container and constraint in a 2-D plane, (b) pendulum model of liquid slosh.

**Table 1.** Parameters of the system.

Parameter	Description	Unit
$m_r$	Total rigid mass including mass of the container and nonsloshing part of liquid	kg
$m_p$	Mass of slosh (mass of pendulum)	kg
$c$	Coefficient of damping	kg · m <sup>2</sup> /s
$l_p$	Length of pendulum	m
$l_o$	Distant between center of rigid mass and point $O$	m
$l_t$	Length of container arm	m
$R$	Radius of cylinder	m
$\beta$	Angle between container handle and rigid mass	rad
$\mathbf{F}_i$	Vector of forces applied by robots to container arm	N
$x$	Position of rigid mass in horizontal direction with respect to base frame $\sum B$	m
$y$	Position of rigid mass in vertical direction with respect to base frame $\sum B$	m
$\alpha$	Angle of the container in vertical direction	rad
$\psi$	Slosh angle or pendulum angle	rad

number of modes increases. Therefore, the fundamental mode can be represented by only a single mass [7]. Hence, as shown in Figure 4(b), the sloshing liquid in a cylindrical container is represented by a rigid liquid mass and a pendulum system. Viscosity and friction between the liquid and the container wall are represented by a damper with a damping constant  $c$ . The necessary parameters for the 2-D system are given in Table 1.

For the 2-D system shown in Figure 4,  $\mathbf{M}_o$ ,  $\mathbf{C}_o$ ,  $\mathbf{G}_o$ ,  $\mathbf{J}_{oi}$ ,  $\mathbf{F}_i$ , and  $\mathbf{X}_o$  are as follows

$$\mathbf{M}_o = \begin{bmatrix} m_r + m_p & 0 & -m_p l_o \cos(\alpha) & m_p l_p \cos(\psi) \\ 0 & m_r + m_p & -m_p l_o \sin(\alpha) & m_p l_p \sin(\psi) \\ -m_p l_o \cos(\alpha) & -m_p l_o \sin(\alpha) & I_r + m_p l_o^2 & -m_p l_o l_p \cos(\alpha - \psi) \\ m_p l_p \cos(\psi) & m_p l_p \sin(\psi) & -m_p l_o l_p \cos(\alpha - \psi) & m_p l_p^2 \end{bmatrix}$$

$$\mathbf{C}_o = \begin{bmatrix} m_p l_o \sin(\alpha) (\dot{\alpha})^2 - m_p l_p \sin(\psi) (\dot{\psi})^2 \\ -m_p l_o \cos(\alpha) (\dot{\alpha})^2 + m_p l_p \cos(\psi) (\dot{\psi})^2 \\ c (\dot{\alpha} - \dot{\psi}) - m_p l_o l_p \sin(\alpha - \psi) (\dot{\psi})^2 \\ -c (\dot{\alpha} - \dot{\psi}) + m_p l_o l_p \sin(\alpha - \psi) (\dot{\alpha})^2 \end{bmatrix}$$

$$\mathbf{G}_o = \begin{bmatrix} 0 \\ (m_r + m_p)g \\ -m_p l_o g \sin(\alpha) \\ m_p l_p g \sin(\psi) \end{bmatrix}$$

$$\mathbf{J}_{o1} = \begin{bmatrix} 1 & 0 & l_c \sin(\alpha - \beta) & 0 \\ 0 & 1 & -l_c \cos(\alpha - \beta) & 0 \end{bmatrix},$$

$$\mathbf{J}_{o2} = \begin{bmatrix} 1 & 0 & -l_c \sin(\alpha + \beta) & 0 \\ 0 & 1 & l_c \cos(\alpha + \beta) & 0 \end{bmatrix}$$

$$\mathbf{X}_o = [x \ y \ \alpha \ \psi]^T, \quad \mathbf{F}_i = [f_{xi} \ f_{yi}]^T$$

Here  $l_c = \sqrt{(l_t + R)^2 + h_G^2}$  is the distance of mass center  $G$  to the robot arm tips. Equations of the motion for the

rigid mass of the container and nonsloshing portion of the liquid are

$$(m_r + m_p)\ddot{x} - m_p l_o \cos \alpha \ddot{\alpha} + m_p l_p \cos \psi \ddot{\psi} + m_p l_o \sin \alpha \dot{\alpha}^2 - m_p l_p \sin \psi \dot{\psi}^2 = f_{x1} + f_{x2} \quad (16)$$

$$(m_r + m_p)\ddot{y} - m_p l_o \sin \alpha \ddot{\alpha} + m_p l_p \sin \psi \ddot{\psi} - m_p l_o \cos \alpha \dot{\alpha}^2 + m_p l_p \cos \psi \dot{\psi}^2 + (m_r + m_p)g = f_{y1} + f_{y2} \quad (17)$$



$$(I_r + m_p l_o^2) \ddot{\alpha} - m_p l_o \cos \alpha \ddot{x} - m_p l_o \sin \alpha \ddot{y} - m_p l_o l_p \cos(\alpha - \psi) \ddot{\psi} - m_p l_o l_p \sin(\alpha - \psi) \dot{\psi}^2 + c(\dot{\alpha} - \dot{\psi}) - m_p l_o g \sin \alpha = \tau_1 + \tau_2 \quad (18)$$

Equation of the motion for the sloshing part of the liquid is

$$m_p l_p^2 \ddot{\psi} + m_p l_p \cos \psi \ddot{x} + m_p l_p \sin \psi \ddot{y} - m_p l_o l_p \cos(\alpha - \psi) \ddot{\alpha} + m_p l_o l_p \sin(\alpha - \psi) \dot{\alpha}^2 - c(\dot{\alpha} - \dot{\psi}) + m_p l_p g \sin \psi = 0 \quad (19)$$

## 5. Numerical results

The expanded impedance control scheme proposed in the previous section was implemented here for the transfer of the liquid in a 2-D plane. The control scheme was carried out using MATLAB/Simulink. Besides, the proposed scheme was simulated, and the results were compared for various conditions. Then, the results were presented for three cases of the transfer of a liquid-filled container, which are as follows:

1. Case 1: without using any control,
2. Case 2: conventional impedance control without a slosh suppression term, and
3. Case 3: expanded impedance control with a slosh suppression term.

Case 1: without using any control means that no feedback control is used to control the position and orientation of the container and liquid slosh. In other words, forces applied to the container handle for transferring the liquid container have not been controlled. That is, the container is moved stepwise from the initial to the final position without implementing any control.

The effect of the slosh suppression term was demonstrated in the simulation. Taking the damping ratio  $\zeta$  for the system between  $0.6 < \zeta < 1$ , the parameters of the impedance controller were chosen as  $\mathbf{M}_{di} = \mathbf{M}_o$ ,  $\mathbf{D}_{di} = \text{diag}[800, 250, 150, 0]$ , and  $\mathbf{K}_{di} = \text{diag}[3000, 1500, 700, 0]$ . Because the effects of slosh mostly occur in the  $x$ -direction in the 2-D motion,  $\mathbf{K}_{d\psi}$  will be considered as  $\mathbf{K}_{d\psi} = [1000, 0, 0, 0]$ . The liquid properties were taken from Bandyopadhyay et al., 2009, and the system parameters used in the simulation are listed in Table 2.

**Table 2.** System parameters.

Parameter	Value	Unit	Parameters	Value	Unit
$m_{ij}$	10	kg	$m_p$	1.32	kg
$l_{ij}$	1.2	m	$m_r$	6	kg
$l_{ij}$	2	kg·m <sup>2</sup>	$c$	$3.049 \times 10^{-4}$	kg·m <sup>2</sup> /s
$l_B$	0.5	m	$l_o$	0.1261	m
$l_t$	0.3	m	$l_p$	0.052126	m
$l_r$	0.0245	kg·m <sup>2</sup>	$\beta$	$\pi/20$	m
$R$	0.095	m	$g$	9.81	m/s <sup>2</sup>

### 5.1. Example I: Rectilinear motion

The desired trajectory for the container mass center  $G$  is set as a straight path from a start point (0, 0.5) to the end point (1.02, 1.52). Maximum acceleration and velocity values are limited to 2 m/s<sup>2</sup> and 0.6 m/s, respectively. The corresponding desired position and acceleration profiles are shown in Figure 5.

For comparison, the results for three cases are shown together in all the figures. As seen in Figure 6, because no control is used in Case 1, the liquid inside the container sloshes freely but is slowly damped down due to viscosity of the liquid (this similar behavior is true for also Example II). The impedance control without the slosh suppression term failed to eliminate the oscillations in the liquid (Case 2). It can be observed that the conventional impedance control was successful to stabilize the container but not the liquid inside the container. However, in the case of the impedance control with the slosh suppression term (Case 3), the motion of the liquid inside the container was also taken as a control parameter; hence, the amplitude of pendulum angle decreased, and the sloshing of the liquid was successfully suppressed in a very short time.

This similar effect can also be observed in the orientation of the container (Figure 6). In the uncontrolled case (Case 1), the sloshing leads to the oscillation of the container. However, in the other cases, the oscillation of the container was reduced by the controller.

The response of the position of the container is shown in Figure 7. In the uncontrolled case, due to the sloshing of the liquid, the container oscillates around the end point (1.02, 1.52). As can be seen in the figure, the effect of the sloshing in  $y$ -direction is quite less in comparison to  $x$ -direction. For both of the controlled cases, the position of the container has been controlled. However, in Case 3, for suppressing the slosh, the container returns to the reference position after

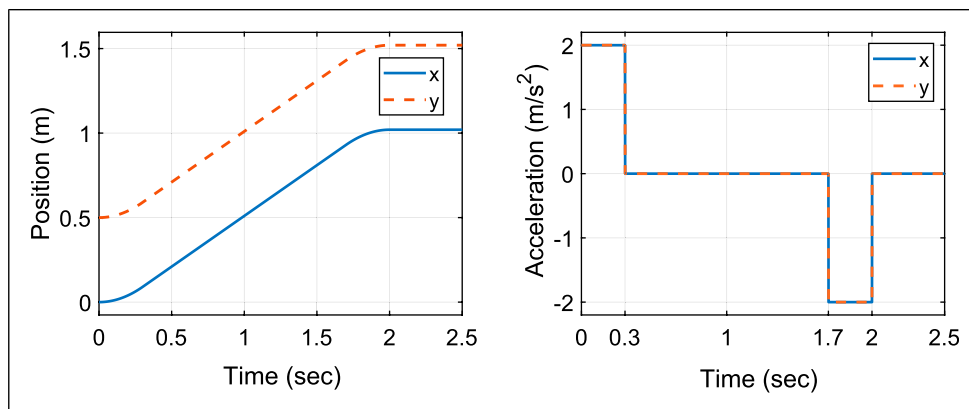


**Figure 5.** Desired trajectory.

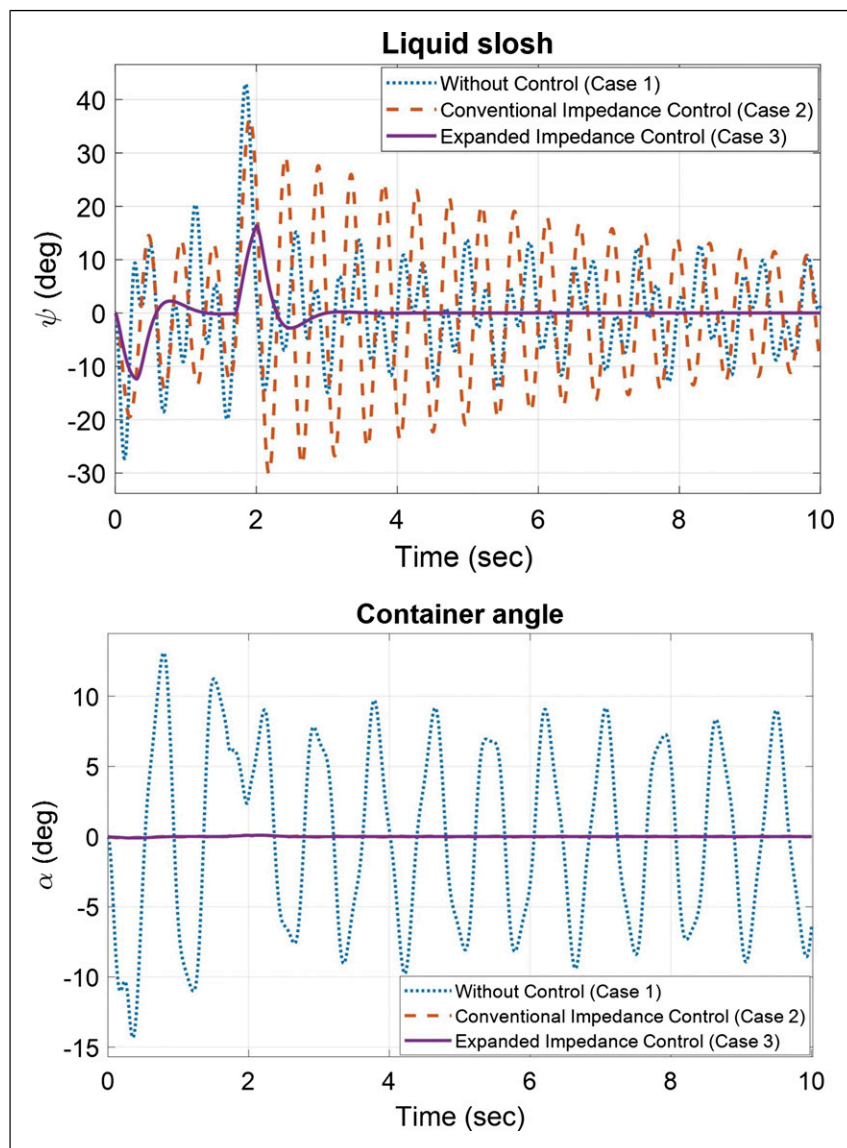


**Figure 6.** Time response of sloshing and container angle.



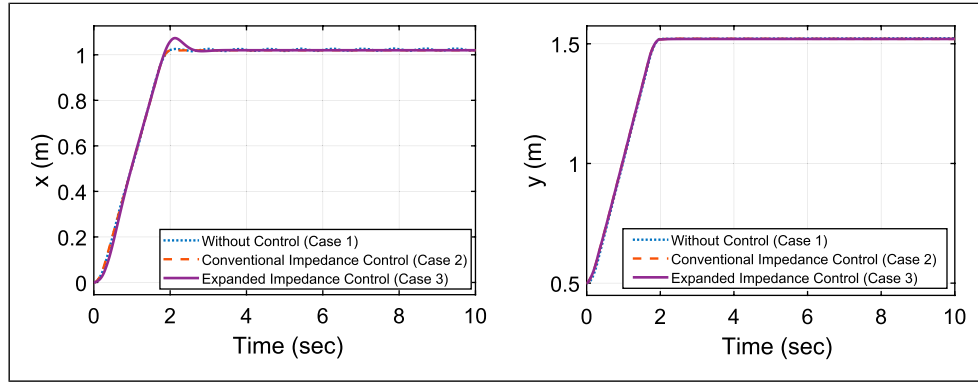


**Figure 7.** Displacement of center of the rigid mass.

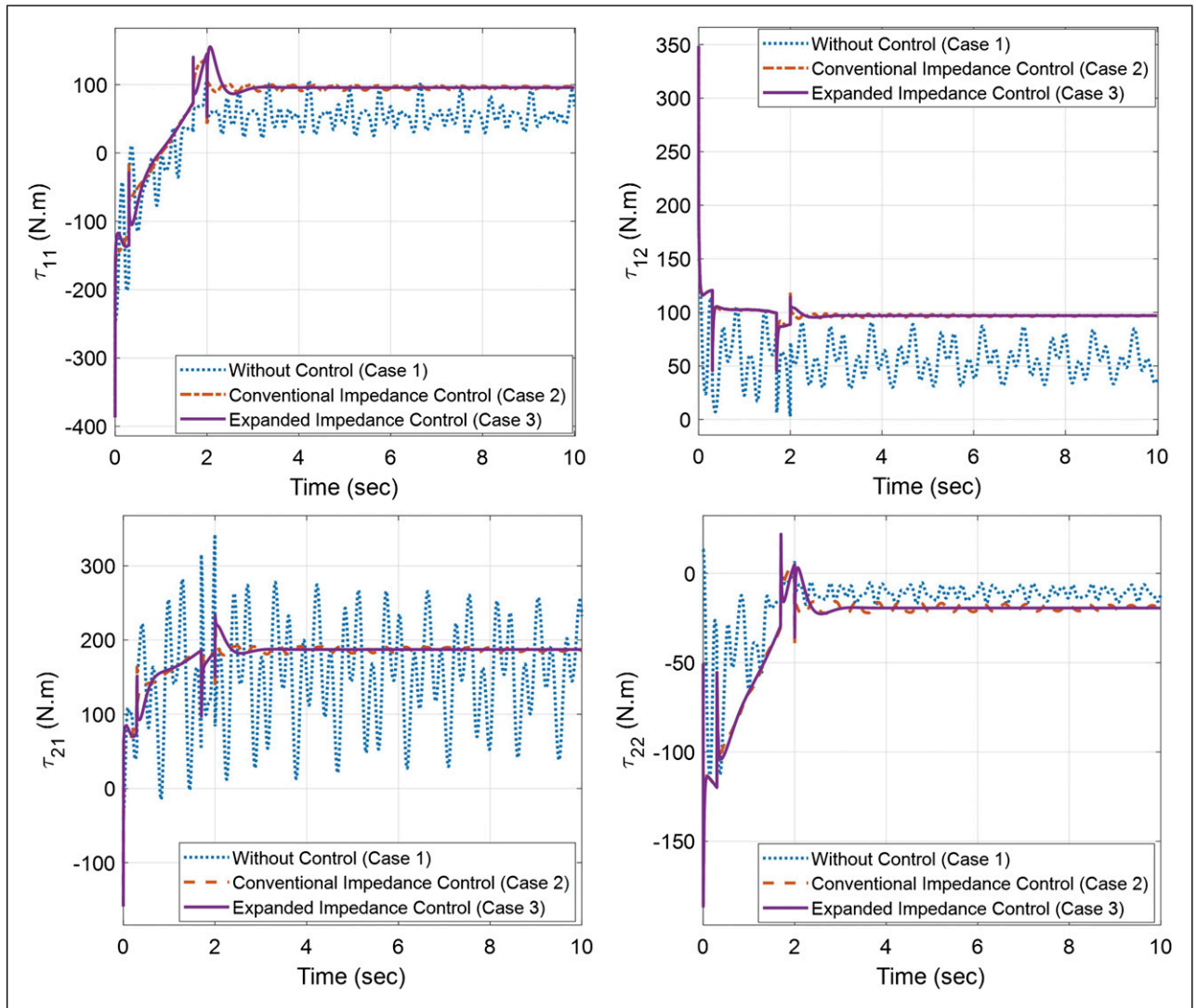


**Figure 8.** Actuator torques.

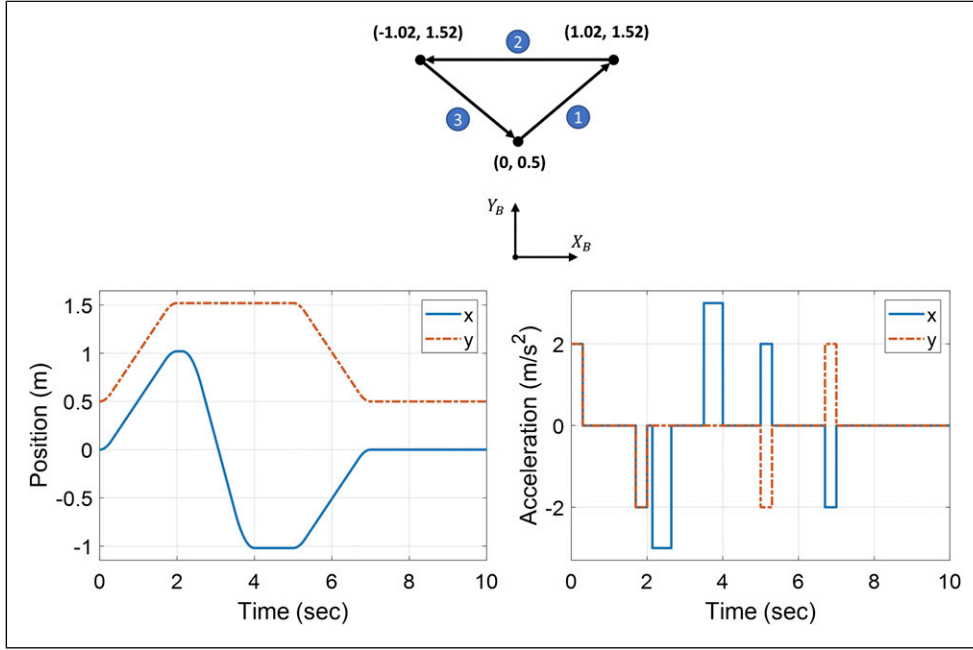


**Figure 9.** Three segmented movement paths with  $(x, y)$  coordinates.

an overshoot of 0.074 m in  $x$ -direction. Figure 8 presents the joint torques of the robots to transfer the liquid-filled container.

### 5.2. Example II: Multiple rectilinear motions

In practice, transferring a liquid container usually takes place as a combination of several movements. Here, we demonstrate the performance of the expanded impedance control for this kind of scenario. As shown in Figure 9, robot movement takes place in three straight path segments. Path 2 has a different acceleration rate from other two paths. The desired values used for acceleration, maximum velocity, and motion start times for each segment are shown in Table 3.

As can be seen from the results, the acceleration and deceleration rates of the container have a direct impact on sloshing. As expected in Path 2, the high acceleration rate leads to more sloshing (Figure 10). Besides, oscillations occur in the container angle due to sloshing. The simulation results also indicate that the impedance control with the slosh suppression term succeeded in suppressing the slosh in all paths. However, while suppressing slosh by the impedance control, some small errors occurred in the position of the container (Figure 11).

**Table 3.** Desired values for path segment.

Path segment	Acceleration (m/s <sup>2</sup> )	Max. vel. (m/s)	Motion start time (s)
1	2	0.6	0
2	3	1.5	2.14
3	2	0.6	5

However, these errors converged to zero rapidly. The variation in the actuator torques during the motion is shown in Figure 12.

Example I was used to demonstrate the main functions of the proposed controller. To avoid mingling with the complexities arisen from the path, the path used in Example I was chosen as simple as possible. However, to test the overall performance of the controller, a more general and challenging profile of the path was used in Example II. Whereas in Example I the transient and steady-state phases of the liquid slosh are clearly distinguished, in Example II, due to discretely connected multiple path segments, there are more than one overlapping transient phases. As mentioned in Sections 5.1 and 5.2, in both examples, the proposed controller is

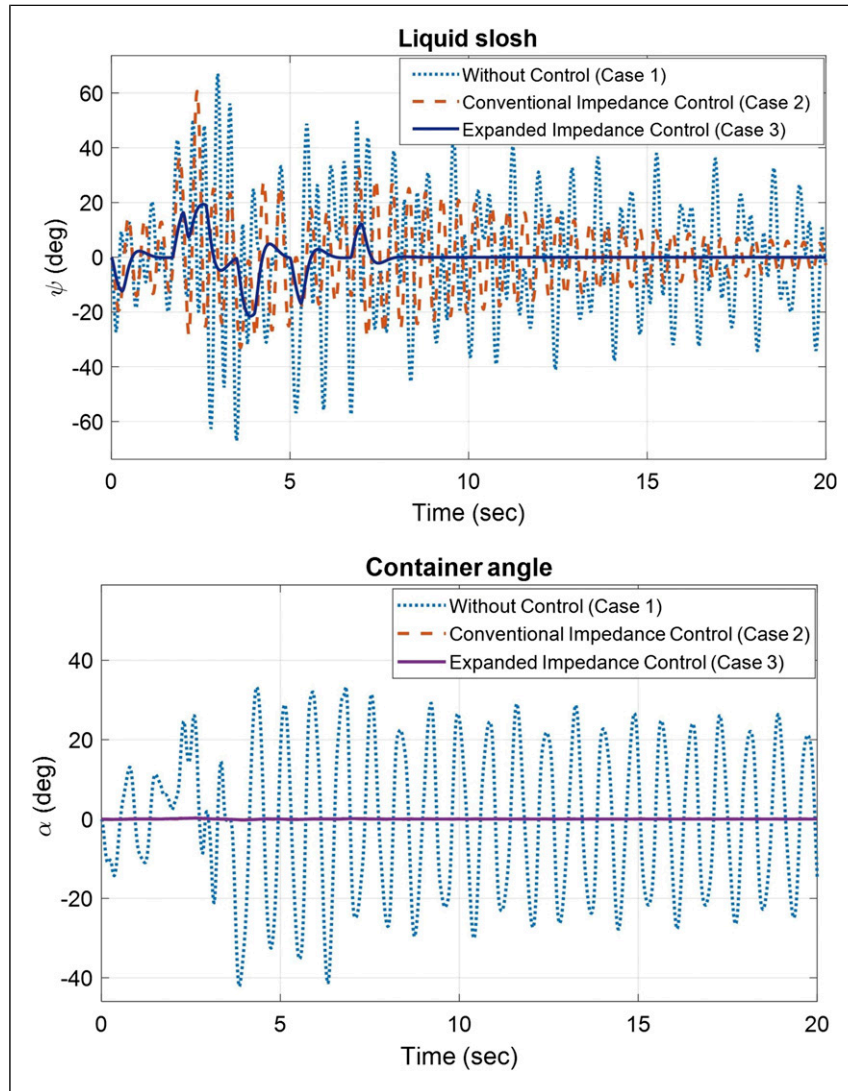


**Figure 10.** Time response of sloshing and container angle.

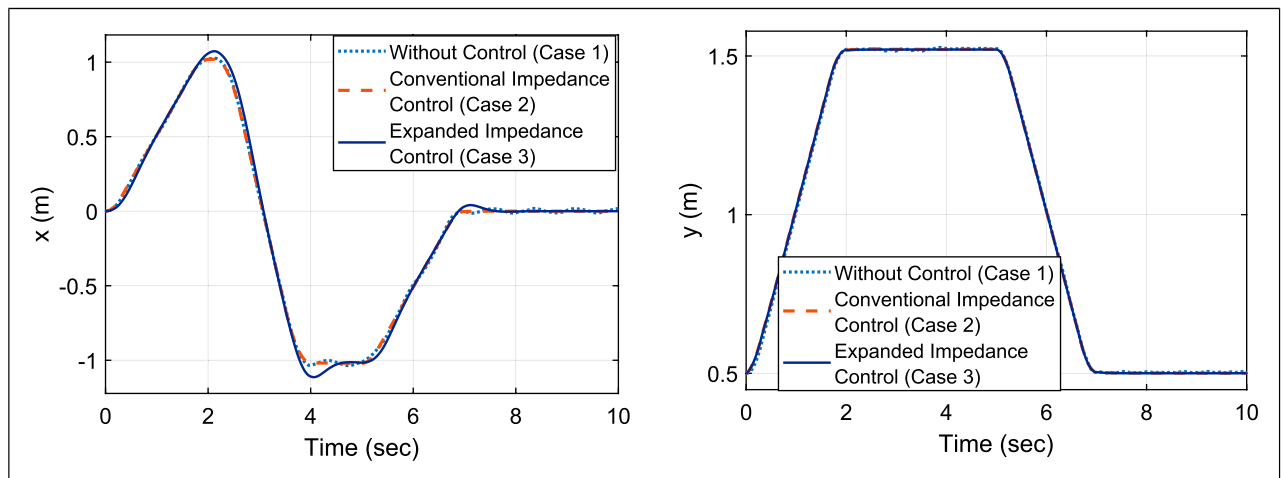


**Figure 11.** Position of center of mass of the container.

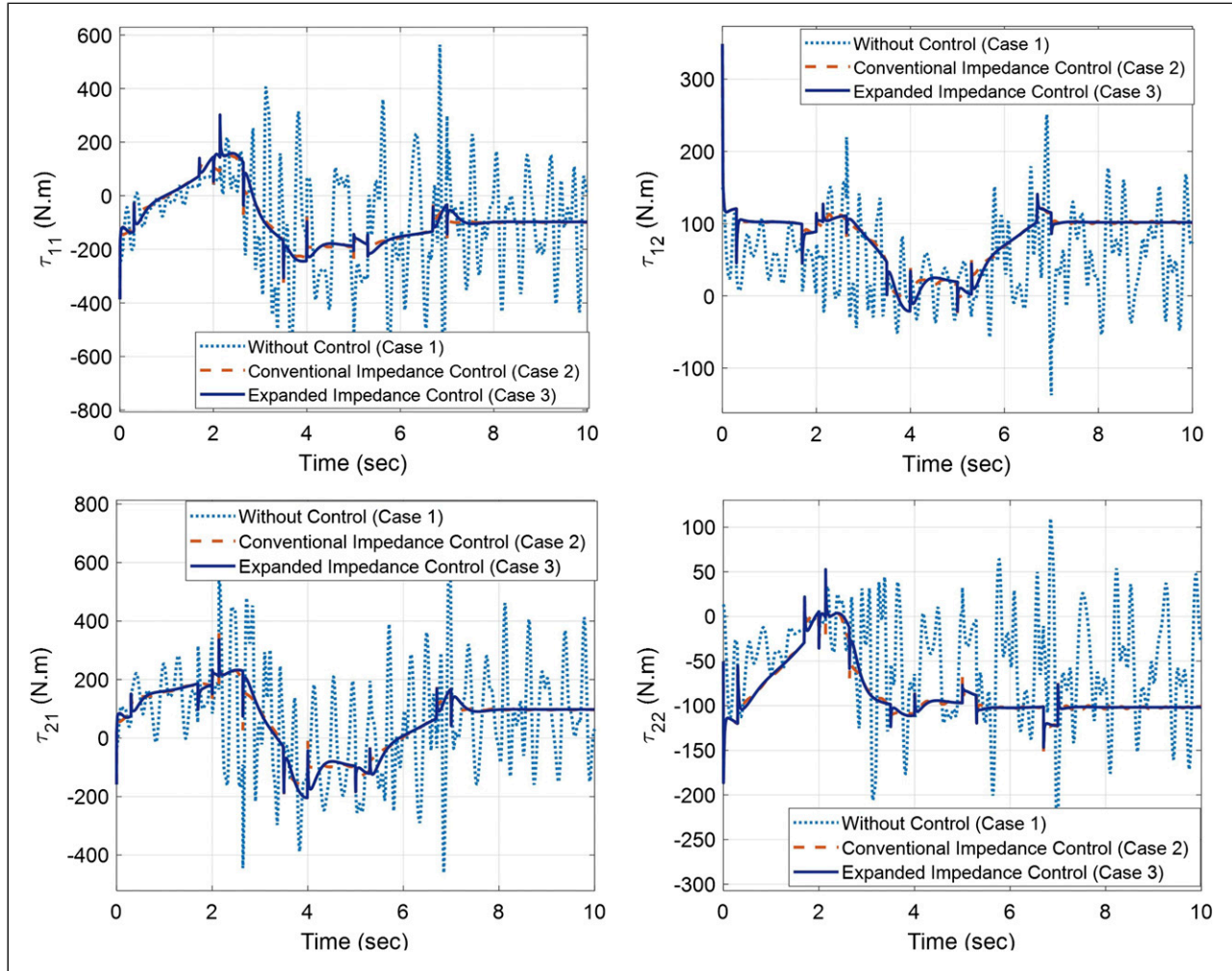


**Figure 12.** Actuator torques.

much faster to suppress the slosh than the conventional impedance control.

## 6. Conclusion

In this study, an expanded impedance control that suppresses sloshing during the transfer of a liquid-filled open container by the dual-arm cooperative robot was proposed. The proposed control algorithm can be used in controlling the safe transport of dangerous liquids via other vehicles as well. The key finding of the current study is that the impedance control is not only able to control rigid and flexible objects but it can also be used to control the passive objects, such as liquids. These results are significant in two important aspects: first, they demonstrate that the conventional impedance control is unsuccessful in suppressing the liquid slosh; second, they indicate that the expanded impedance control effectively suppresses the slosh and prevents liquid spilling from the container.

The effectiveness of the proposed controller was demonstrated by two separate examples. In the first example, the liquid container is transferred in a single rectilinear movement, whereas in the second example, it is transferred in several discretely combined movements, and hence exposed to sudden acceleration and deceleration. It was shown that the conventional impedance control is successful to stabilize the container but not the liquid inside the container, whereas the expanded impedance control works successfully in both controlling the container position and suppressing the liquid slosh. In Example I, while in the conventional impedance control (Case2), the maximum slosh amplitude reaches  $34.8^\circ$ , and in the expanded impedance control (Case3), the maximum slosh amplitude remains at only  $18.72^\circ$ . This means that the slosh of the liquid decreased down to about 46% by the proposed expanded impedance control. Furthermore, in Case 2, the system reaches the steady state after 44 s, whereas in Case 3, the time to reach the steady state is only



3.9 s. This similar improvement is observed in Example II as well.

A major downside of the proposed controller is that while trying to suppress the slosh, it causes certain overshoot in the position of the liquid-filled container during the acceleration and deceleration phases, which is not the case in the conventional impedance control. However, this overshoot is relatively small and takes a very short time and does not cause any spillover for the liquids with adequate viscosities.

### Declaration of conflicting interests

The author(s) declared no potential conflicts of interest with respect to the research, authorship, and/or publication of this article.

### Funding

The author(s) received no financial support for the research, authorship, and/or publication of this article.

### ORCID iDs

Babak Naseri Soufiani  <https://orcid.org/0000-0001-6007-3875>  
Mehmet Arif Adli  <https://orcid.org/0000-0002-3223-064X>

### References

- Adli MA and Hanafusa H (1993) Compliance control and selective compliance center via internal forces in redundantly actuated closed chain mechanisms. *Transactions of the Society of Instrument and Control Engineers(SICE)* 29(3): 253–262.
- Adli MA, Ito K and Hanafusa H (1995) Controlling the contact compliance via internal forces on objects held by dual-arm robots. In: IROS 95–1995 IEEE/RSJ international conference on intelligent robots and systems: human robot interaction and cooperative robots proceedings, Pittsburgh, PA, 5–9 August 1995, Vol. 1, 62–69. Washington, DC: IEEE.
- Adli MA, Nagai K, Miyata K, et al. (1991) Analysis of internal force effect in parallel manipulators. *Transactions of the Society of Instrument and Control Engineers(SICE)* 27(11): 1266–1273.
- Akdoğan E and Adli MA (2011) The design and control of a therapeutic exercise robot for lower limb rehabilitation: Physiotherabot. *Mechatronics* 21(3): 509–522.
- Al-Yahmadi AS, Abdo J and Hsia T (2007) Modeling and control of two manipulators handling a flexible object. *Journal of the Franklin Institute* 344(5): 349–361.
- Aribowo W, Yamashita T, Terashima K, et al. (2010) Input shaping control to suppress sloshing on liquid container transfer using multi-joint robot arm. In: 2010 IEEE/RSJ international conference on intelligent robots and systems, Taiwan, 18–22 October 2010, pp. 3489–3494. IEEE.
- Bandyopadhyay B, Gandhi P and Kurode S (2009) Sliding mode observer based sliding mode controller for slosh-free motion through PID scheme. *IEEE Transactions on Industrial Electronics* 56(9): 3432–3442.
- Caccavale F, Chiacchio P, Marino A, et al. (2008) Six-DOF impedance control of dual-arm cooperative manipulators. *IEEE/ASME Transactions on Mechatronics* 13(5): 576–586.
- Hamaguchi M, Terashima K and Nomura H (1994) Optimal control of liquid container transfer for several performance specifications. *Journal of Advanced Automation Technology* 6: 353–360.
- Hasheminejad SM, Mohammadi M and Jarrahi M (2014) Liquid sloshing in partly-filled laterally-excited circular tanks equipped with baffles. *Journal of Fluids and Structures* 44: 97–114.
- Hu J, Hou Z, Zhang F, et al. (2012) Training strategies for a lower limb rehabilitation robot based on impedance control. In: 2012 Annual international conference of the IEEE engineering in medicine and biology society, San Diego, CA, 28 August–1 September 2012, pp. 6032–6035. IEEE.
- Ibrahim RA (2005) Liquid sloshing dynamics: theory and applications. New York: Cambridge University Press.
- Jung J, Yoon H, Lee C, et al. (2012) Effect of the vertical baffle height on the liquid sloshing in a three-dimensional rectangular tank. *Ocean Engineering* 44: 79–89.
- Kim DH and Choi JW (2000) Attitude controller design for a launch vehicle with fuel-slosh. *SICE 2000*. In: Proceedings of the 39th SICE annual conference. international session papers, Japan, 28–28 July 2000, pp. 235–240. IEEE.
- Kurode S, Spurgeon SK, Bandyopadhyay B, et al. (2013) Sliding mode control for slosh-free motion using a nonlinear sliding surface. *IEEE/ASME Transactions on Mechatronics* 18(2): 714–724.
- Moosavian SAA and Papadopoulos E (2010) Cooperative object manipulation with contact impact using multiple impedance control. *International Journal of Control, Automation and Systems* 8(2): 314–327.
- Naseri Soufiani B and Adli MA (2020) Pole placement and LQR control of slosh-free liquid transportation with dual-arm cooperative robot. *Journal of the Faculty of Engineering & Architecture of Gazi University* 35(4): 2255–2267.
- Panigrahy P, Saha U and Maity D (2009) Experimental studies on sloshing behavior due to horizontal movement of liquids in baffled tanks. *Ocean Engineering* 36(3): 213–222.
- Pridgen B, Bai K and Singhose W (2010) Slosh suppression by robust input shaping. In: 49th IEEE conference on decision and control (CDC), Atlanta, GA, 15–17 December 2010, pp. 2316–2321. IEEE.
- Ren Y, Liu Y, Jin M, et al. (2016) Biomimetic object impedance control for dual-arm cooperative 7-DOF manipulators. *Robotics and Autonomous systems* 75: 273–287.
- Reyhanoglu M and Hervas JR (2012) Nonlinear dynamics and control of space vehicles with multiple fuel slosh modes. *Control Engineering Practice* 20(9): 912–918.
- Reyhanoglu M and Hervas JR (2013) Nonlinear modeling and control of slosh in liquid container transfer via a PPR robot. *Communications in Nonlinear Science and Numerical Simulation* 18(6): 1481–1490.
- Smith C, Karayiannidis Y, Nalpantidis L, et al. (2012) Dual arm manipulation—A survey. *Robotics and Autonomous systems* 60(10): 1340–1353.
- Thakar PS, Bandyopadhyay B, Gandhi P, et al. (2012) Robust control of rotary slosh using integral sliding modes. In: 2012 12th International workshop on variable structure systems (VSS), Mumbai, Maharashtra, 12–14 January 2012, pp. 440–445. IEEE.
- Tsoi YH and Xie SQ (2009) Impedance control of ankle rehabilitation robot. In: 2008 IEEE international conference on

- robotics and biomimetics, Bangkok, Thailand, 22–25 February 2009, pp. 840–845. IEEE.
- Tzamtzi MP, Koumboulis FN and Kouvakas ND (2007) A two stage robot control for liquid transfer. In: 2007 IEEE conference on emerging technologies and factory automation (EFTA 2007), Patras, Greece, 25–28 September 2007, pp. 1324–1333. IEEE
- Wang M, Luo M, Li T, et al. (2015) A unified dynamic control method for a redundant dual arm robot. *Journal of Bionic Engineering* 12(3): 361–371.
- Xue M-A, Zheng J and Lin P (2012) Numerical simulation of sloshing phenomena in cubic tank with multiple baffles. *Journal of Applied Mathematics* 2012: 1–21.
- Yano KI and Terashima K (2001) Robust liquid container transfer control for complete sloshing suppression. *IEEE Transactions on Control Systems Technology* 9(3): 483–493.
- Yoshikawa T (1990) *Foundations of Robotics: Analysis and Control*. Cambridge, London: MIT press.